

Scenario generation for market risk models using generative neural networks

Solveig Flaig*[†], Gero Junike[‡]

06.09.2021

Abstract

In this research, we show how to expand existing approaches of generative adversarial networks (GANs) being used as economic scenario generators (ESG) to a whole internal model - with enough risk factors to model the full band-width of investments for an insurance company and for a one year horizon as required in Solvency 2. For validation of this approach as well as for optimisation of the GAN architecture, we develop new performance measures and provide a consistent, data-driven framework. Finally, we demonstrate that the results of a GAN-based ESG are similar to regulatory approved internal models in Europe. Therefore, GAN-based models can be seen as an assumption-free data-driven alternative way of market risk modelling.

Keywords Generative Adversarial Networks, Economic Scenario Generators, nearest neighbour distance, market risk modelling, Solvency 2

1 Extended Abstract

Insurance companies calculating market risk under Solvency 2 with an internal model are obliged to generate financial market scenarios. Traditionally, this is solved by using a Monte-Carlo simulation with financial mathematical models in an economic scenario generator (ESG). We present here Generative Adversarial Networks (GANs) as an alternative solution. GANs are widely used in image generation, but, to the best of our knowledge for the first time, we implement GANs for scenario generation and for a complete Solvency 2 market risk calculation. For optimization of the GAN infrastructure, hyperparameter

*Corresponding author. Deutsche Rückversicherung AG, Kapitalanlage / Marktrisikomanagement, Hansaallee 177, 40549 Düsseldorf, Germany. E-Mail: solveig.flaig@deutscherueck.de.

[†]Carl von Ossietzky Universität, Institut für Mathematik, 26111 Oldenburg, Germany.

[‡]Carl von Ossietzky Universität, Institut für Mathematik, 26111 Oldenburg, Germany. E-Mail: gero.junike@uol.de.

optimization and validation, we develop new performance measures and provide a consistent, assumption-free framework for the evaluation of the scenario generation. The main properties of these evaluation measures, mainly based on nearest-neighbour distances, are presented. Finally, we compare the results of a GAN-based ESG to the classical ESG approach. For this comparison, we use the benchmark portfolios created by the European Insurance and Occupational Pensions Authority (EIOPA) for the market and credit risk comparison study (MCRCS). Those portfolios are available for asset- and liability side and represent average exposure profiles of insurance companies in Europe. The comparison shows that the GAN-based ESG leads to similar results than the current approaches used in regulatory approved internal market risk models in Europe. In comparison to the currently used ESGs, they have the advantage that they are assumption-free, are able to model more complex dependencies, have no need of a time-consuming calibration process and can include new risk factors easily.

2 Introduction

The generation of realistic scenarios how the financial markets could behave in the future is one key component of internal market risk models used by insurance companies for Solvency 2 purposes. Currently, this is done using economic scenario generators (ESGs) which are mainly based on financial mathematical models, see Bennemann [2011] and Pfeifer and Ragulina [2018]. These ESGs need strong assumptions on the behaviour of the risk factors and their dependencies, are time-consuming to calibrate and it is difficult in this framework to model complex dependencies.

An alternative method for scenario generation can be a type of neural networks called generative adversarial networks (GANs), invented by Goodfellow et al. [2014]. This is a network architecture consisting of two neural networks which has gained a lot of attention due to their ability to generate real-looking pictures, see Aggarwal et al. [2021]. According to Motwani and Parmar [2020] and Li et al. [2020], GANs are one of the dominant methods for the generation of realistic and diverse examples in the domains of computer vision, image generation, image style transfer, text-to-image-translations, time-series synthesis and natural language processing.

As financial data, at least for liquid instruments, is consistently available, GANs are used in various fields of finance, including market prediction, tuning of trading models, portfolio management and optimization, synthetic data generation and diverse types of fraud detection, see Eckerli [2021]. Henry-Labordere [2019], Lezmi et al. [2020], Fu et al. [2019], Wiese et al. [2019], Ni et al. [2020] and Wiese et al. [2020] have already used GANs for scenario generation in the financial sector. The focus of their research was the generation of financial time series for a limited number of risk factors (up to 6) and / or a single asset class.

To the best of our knowledge, there is no research performing a full value-at-risk calculation for an insurance portfolio based on these scenarios.

The validation of the GAN performance was mainly carried out visually or with a few statistic parameters, e.g. in Wiese et al. [2019], Ni et al. [2020] and Wiese et al. [2020]. However, a data-driven assessment of the quality of the generated scenarios is desirable from two points of view: to validate the model on the basis of Solvency 2 and to optimise the hyperparameters of the GAN and its architecture. In particular, measures based on nearest neighbor distances, as studied by Cover and Hart [1967], Bickel and Breiman [1983], Henze [1988], Mondal et al. [2015] and Ebner et al. [2018] seem suitable.

In this research we

- expand the scenario generation by a GAN to a complete risk calculation serving for Solvency 2 purposes in insurance companies
- provide a consistent, assumption-free framework for the evaluation of the scenario generation including the evaluation of dependencies between risk factors and the detection of a memorizing effect
- compare the results of a GAN-based ESG to the classical ESG approach implemented in regulatory approved market risk models in Europe.

The paper is structured as follows: In Section 3, we provide some background both on market risk calculation under Solvency 2 and on GANs. Section 4 recalls some measures from literature and presents new measures to evaluate GANs. Additionally, we present here a framework how to combine these measures in a hyperparameter and architecture optimization process. EIOPA annually conducts a benchmarking exercise for approved market risk models in Europe, called MCRCs. This study together with a comparison of the results of a GAN-based ESG to the results in the study can be found in Section 5. Section 6 concludes.

3 Background

Before we present our work, we will give a short introduction to the two main topics involved: economic scenario generators (ESG) and their use for Solvency 2 market risk calculation and generative adversarial networks (GAN).

3.1 Market risk calculation under Solvency 2

In 2016, a new regulation for insurance companies in Europe was introduced: Solvency 2. One central requirement is the calculation of the solvency capital requirement, called SCR. The SCR represents the risk of the insurer. The eligible capital of an insurance company is then compared with the SCR to determine whether the eligible capital is sufficient to cover the risk taken by the insurance

company.

The solvency capital requirement equals the Value-at-Risk (VaR) at a 99.5%-level for a time horizon of 1 year. A mathematical definition of the VaR and a derivation of its usage in this context can be found in Denuit et al. [2006, p. 69].

The risk of an insurer can be divided in different modules: market risk, counterparty default risk, life underwriting risk, health underwriting risk, non-life underwriting risk and operational risk. The modules themselves consist of sub-modules, as Figure 3.1, taken from EIOPA [2014], shows:

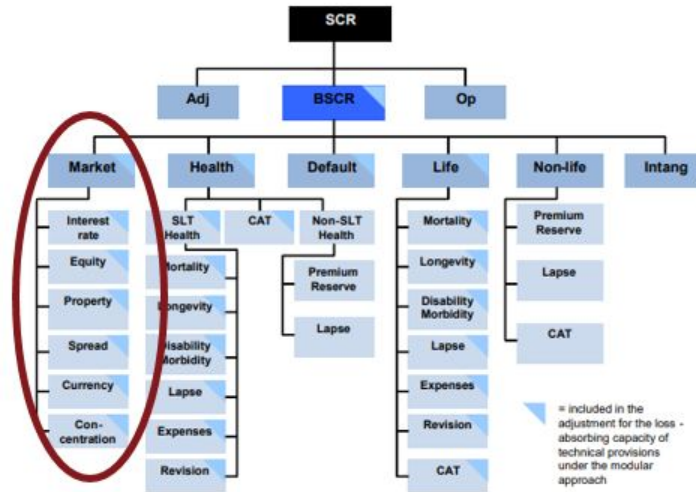


Figure 3.1: Modules of the Solvency 2 standard formula, see EIOPA [2014, p. 6]

The SCR can be calculated using either the standard model or an internal model. For the standard model, the regulatory framework, European Union [2015], sets specific rules for the calculation for each risk encountered by the insurance company. Each internal model has to cover the same types of risks as the standard model and must be approved by local supervisors to ensure accordance with the principles of Solvency 2.

In this work, we will focus on the calculation of the market risk of a non-life insurer, covering the submodules interest rate, equity, property, spread, currency and concentration risk. However, the methods can be applied for other risks, too. The reason for selecting market risk here is twofold:

- the underlying data in the financial market is publicly available and equal for all insurers and

- a comprehensive benchmark exercise, called “market and credit risk comparison study” MCRCS conducted by the “European Insurance and Occupational Pensions Authority” EIOPA is available for comparison of the results.

We selected a non-life insurer because in contrast to a life insurer, there is no direct dependency between asset and liability side. This is the case in the MCRCS study, too. However, a GAN-based ESG can be used in the market risk calculation of a life insurer, too, as they also employ ESGs in the simulations.

Currently, internal models for market risk often use Monte-Carlo simulation techniques to derive the risk of the (sub)modules and then use correlations or copulas for aggregation, see Bennemann [2011, p. 189] and Pfeifer and Ragulina [2018]. The basis of the Monte-Carlo simulation is a scenario generation performed by an “economic scenario generator” ESG. This ESG implements financial-mathematical models for all relevant risk factors (e.g. interest rate, equity) and their dependencies. Under those scenarios, the investment and liabilities portfolio of the insurer is evaluated and the risk is given by the 0.5%-percentile of the loss in these scenarios.

3.2 Generative adversarial networks

Generative adversarial networks, called GANs, are an architecture consisting of two neural networks which are used to play a minimax-game. In 2014, GANs were introduced by Goodfellow et al. [2014] and have gained a lot of attention afterwards because the promising results especially in image generation. A good introduction to GANs can be found in Goodfellow et al. [2014], Goodfellow [2016] and Chollet et al. [2018]. According to Motwani and Parmar [2020] and Li et al. [2020], GANs are one of the dominant methods for the generation of realistic and diverse examples in the domains of computer vision, image generation, image style transfer, text-to-image-translations, time-series synthesis, natural language processing, etc.

Other popular methods for the generation of data based on empirical observations are variational autoencoders and fully visible belief networks, see Goodfellow [2016, p. 14]. However, we will use GANs here, as “GANs are generally regarded as producing better samples”, see Goodfellow [2016, p. 14].

For the mathematical discussion in the remainder of this section, we use the following notations:

Let $(\Omega, \mathcal{F}, \mathbb{P})$ be a probability space and $d \in \mathbb{N}$ the number of risk factors that we model. In this research, we used a set of $d = 46$ risk factors. The list of those risk factors can be found in Appendix D. $E : \Omega \rightarrow \mathbb{R}^d$ denotes the random vector of the empirical data, the generated data by a GAN is described by the random vector $G : \Omega \rightarrow \mathbb{R}^d$. Let being $E_j, j \in \{1, \dots, m\}$, $m \in \mathbb{N}$, be independent copies

of the random vector E and $G_j, j \in \{1, \dots, m\}$ independent copies of the random variable G . Let $\mathbb{E}(\omega) = \{E_1(\omega), \dots, E_m(\omega)\}$ and $\mathbb{G}(\omega) = \{G_1(\omega), \dots, G_m(\omega)\}$ be sets of those random variables for each $\omega \in \Omega$. The idea of a GAN is that the generated data G should follow the same (but unknown) distribution as the empirical data.

Technically, a GAN consists of two neural networks, named *generator* and *discriminator*. The discriminator network is trained to distinguish real datapoints from “fake” datapoints and assigns every given datapoint a probability that this datapoint is real. The input to the generator network is random noise coming from a so called *latent space*. The generator is trained to produce datapoints that look like real datapoints and would be classified by the discriminator as being real with a high probability. Picture 3.2, taken from Chen et al. [2018, p. 2], illustrates the general architecture of a GANs training procedure:

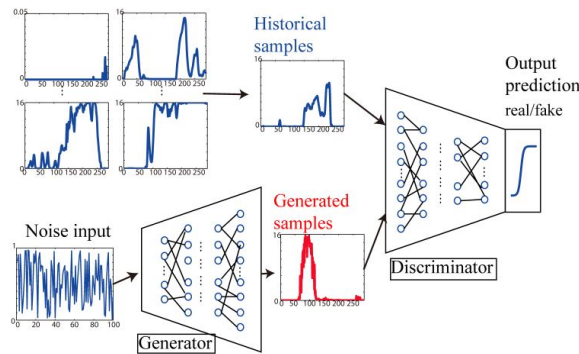


Figure 3.2: Architecture of GANs training procedure, according to Chen et al. [2018]

A GAN training process consists of several iterations where the weights of both neural networks are optimised until the data from the generator is close to the empirical/historical data. This evolution during training can be visualised in case of a two-dimensional data distribution in Picture 3.3. The red data here represents the empirical data to be learned whereas the blue data is generated at the current stage of training of the generator. One can clearly see that the generated data matches the empirical data more closely when more training iterations of the GAN have taken place.

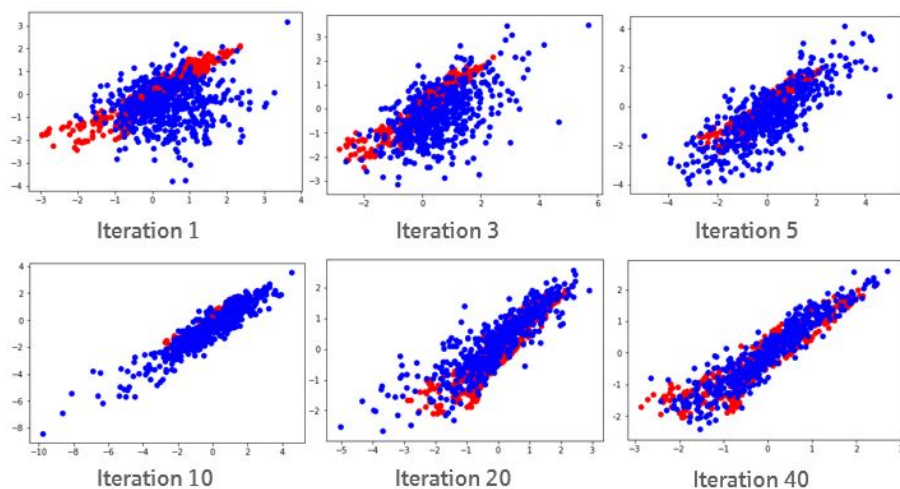


Figure 3.3: Scatterplots of the training iterations of a GAN for a two-dimensional data distribution, red = empirical data, blue = generated data

3.3 Application of a GAN as an ESG

The strength of GANs is especially what ESGs should be good at - producing samples of an unknown distribution based on empirical examples of that distribution. Therefore, we will apply a GAN as an ESG.

As shown in Chen et al. [2018], a GAN can be used to create new and distinct scenarios that capture the intrinsic features of the historical data. Fu et al. [2019, p. 3] already noted in their paper that a GAN, as a non-parametric method, can be applied to learn the correlation and volatility structures of the historical time series data and produce unlimited real-like samples that have the same characteristics as the empirical observed time-series. Fu et al. [2019, Chapter 5] have tested that this works with two stocks and calculated a 1-day VaR.

In our work here, we demonstrate how to expand this to a whole internal model - with enough risk factors to model the full band-width of investments for an insurance company and for a one year horizon as required in Solvency 2. Diagram 3.4 compares schematically the classical ESG and the idea of a GAN-based ESG and illustrates how this simplifies the ESG process.

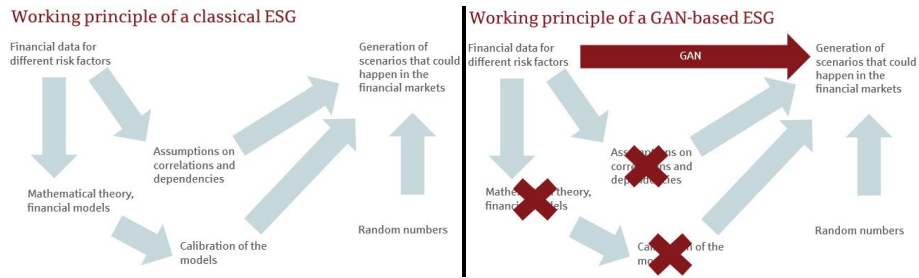


Figure 3.4: Comparison of the working principles of a classical and a GAN-based ESG

The main advantages of a GAN-based ESG, compared to a classical ESG, are:

- *Assumption-free*: A GAN-based ESG can be seen as being assumption-free as it does not contain any financial assumptions regarding distributions of the risk factors and their dependencies. All information on the risk factors stems directly from the empirically observed data. Assumptions that are enforced by models and that have proven to be wrong afterwards, e.g. the assumption of interest-rates not becoming negative that was popular until the financial crisis 2008/2009, can therefore not lead to a wrong risk-assessment.
- *Modelling of dependencies*: As Denuit et al. [2006, Chapter 4] explains, the modelling of dependence structures beyond multivariate normality has become crucial in financial applications. In modern risk models, dependencies are often modelled using copulas. A certain copula has to be selected for each risk-factor and must be fitted so that the desired dependencies are reached. In practice, the modelling of dependencies is very difficult. In a GAN-based model, the dependencies are automatically incorporated from the empirical data.
- *No need for a calibration process*: Calibration of the financial models to match the empirical data is a task that has to be performed regularly by risk managers to keep the models up to date. This is a cumbersome process and there is no standard process for calibration, see DAV [2015, Chapter 2.1]. This task is not needed for GAN-based models and makes them easier to use. If new data shall be included, the GAN simply has to be fed with the new data.
- *Easy integration of new risk factors*: While the integration of new risk factors in classical ESGs often poses several issues and is quite laborious, in a GAN-based model, expansions of a GAN to include more risk-factors are straightforward.

A disadvantage of a GAN-based ESG is the fact that it purely relies on events that have happened in the past in the financial markets and cannot e.g. produce of new dependencies that are not included in the data the model is trained with. Classical financial models aim to derive a theory based on developments in the past and can therefore probably produce scenarios a GAN cannot come up with.

It is probable that a GAN-based ESG adapts faster to a regime-switch in one of the risk factors of the model: In a classical ESG a new financial model has to be developed and implemented, whereas a GAN has just to be trained with new data.

4 GAN evaluation measures for GAN-based ESGs

When a GAN is used for scenario generation, the suitability of the generated scenarios of the GAN has to be evaluated, i.e. whether the generated scenarios sufficiently matches the empirical observed data. This is important for validation purposes as well as to optimize the GAN infrastructure and the hyperparameters of the two neural networks, generator and discriminator.

For example, Figure 4.1 shows the results of the GAN scenario generation after only a few iterations (left) and after a sufficient amount of training iterations (right). The red data in these figures represents the empirical data whereas the blue resp. green points represent generated data. GAN evaluation measures should assign a clear and robust value to each scenario generation attempt representing the goodness-of-fit between empirical and generated data. In these cases, the evaluation measure should assign a better value to the scenarios on the right than to those on the left.

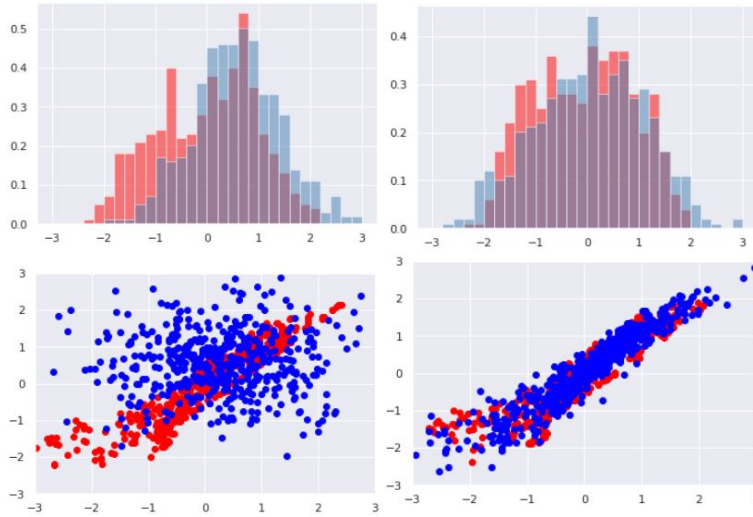


Figure 4.1: Comparison of histograms and scatterplots after a few (left) and after sufficient (right) training iterations, red = empirical data, blue = generated data

In this research, we employ a pure-data driven evaluation approach as one of the main advantages of using a GAN for scenario generation is that no further (financial-mathematical) assumptions on e.g. distributions are necessary and therefore we do not want to use assumptions in the evaluation. Furthermore, we want to take measures that are easily interpretable so they can also be used for validation purposes in Solvency 2.

The suitability of the scenarios can be divided into three categories:

- (1) the alignment between the distributions of empirical observation and generated data for each risk factor
- (2) the alignment of the dependencies between empiric and generated data, i.e. the generated points are near the empirical ones and the GAN does not suffer from “mode collapse”, i.e. all areas of empiric data points are covered by generated data points
- (3) the GAN is not “overfitted” and creates new scenarios instead of memorizing empirical ones.

These three points are discussed in Sections 4.1, 4.2 and 4.3, respectively.

4.1 *Measure for the alignment of the distributions: Wasserstein distance*

The Wasserstein distance is commonly used to calculate the distance between two probability distribution functions. In our case of a one dimensional issue (empirical distribution functions for each risk factor), we can use the univariate Wasserstein distance to calculate the distance between the two density functions of E and G . The definition of the Wasserstein distance can be found e.g. in Hallin et al. [2021, p. 5].

The *Wasserstein distance* is also known as earth-mover-distance as it can be interpreted as the minimal amount of earth that has to be moved to transform the two probability measures into each other. In terms of validation, the Wasserstein distance in one dimension can be rewritten as a difference between the quantile functions. Therefore, as Ramdas et al. [2017, Chapter 4.3], states Wasserstein is a QQ-test which is often used in validation of internal models and therefore fits for our purpose.

4.2 *Measure for the alignment of the dependencies between empiric and generated data: non-covered ratio*

The test on the alignment of the dependencies of the empiric and generated data can be reformulated as a multivariate two-sample test where we want to test the equality of two multivariate distributions based on two sets of independent observations.

We found the following tests in literature, which can be applied in our context:

- the number of statistically different bins from Richardson and Weiss [2018] as mentioned in Borji [2019],
- nearest neighbor coincidences from Mondal et al. [2015]
- Wald-Wolfowitz two-sample test adapted from Friedman and Rafsky [1979].

We, however, propose a new measure which is easily interpretable, the *non-covered ratio*. This measure is inspired by the work of Henze [1988] and Mondal et al. [2015].

First, we want to give some illustrative understanding of the new measure *non-covered ratio* which can be interpreted easily as a measure on multidimensional scatterplots. The idea is that for a good fit between empirical data E and generated data G , in every “near neighbourhood” of an empiric datapoint E_j , there should be a generated datapoint G_i , too, and vice versa. A data point in

this context is defined as being in the “near neighborhood”, if it is closer than the k -nearest neighbor of E_j out of all empirical data points. Before defining this formally, we will have a look at an example and discuss why we will use this measure instead of utilizing existing ones.

In the two visual examples in Figure 4.2 (for $k = 1$), we drew three empirical data points E_i and three generated data points G_j . In the figures, we denoted the 1-nearest neighbor distance of a data point E_i to all other empirical data points by R_i .

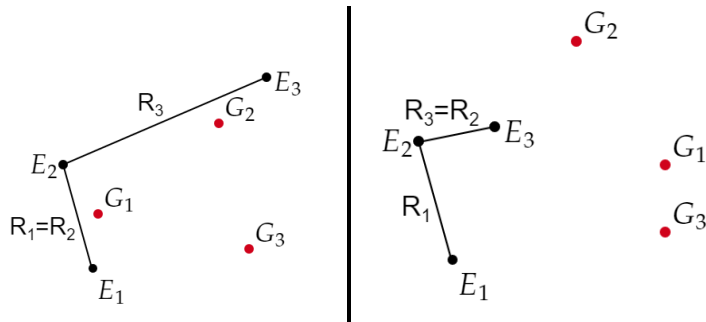


Figure 4.2: Examples for the definition of the non-covered ratio

In the left figure, for all empirical datapoints E_i there is a generated data point G_j which is closer than the nearest neighbor out of \mathbb{E} . Therefore, the non-covered ratio equals 0. In the right figure, however, all generated datapoints G_j are further away from each E_i than the nearest neighbor out of the empirical set. So, the non-covered ratio equals 1. As we can see, this measure is easily interpretable and is aligned with the notion of a good match.

We decided to use the non-covered ratio instead of the other measures mentioned above for the following qualitative reasons. The number of statistically different bins from Richardson and Weiss [2018] in our tests does not converge smoothly, therefore we excluded it from our selection.

- It is the most relaxed measure in the comparison
- Areas with a bad match cannot be compensated with areas with a very close match

Most relaxed in this context means that with this measure more deviations between the two data sets are accepted than for the other measures. In the non-covered ratio, there only has to exist one generated data point being inside the k -nearest neighbor ball of E_i for this ratio to be at its minimal value. The “nearest neighbor coincidences” test, in contrast, requires half of the generated points to be inside the k -nearest neighbor ball of E_i to be at its minimal value.

The Wald-Wolfowitz test is most strict: It does not only require half of the generated data points to be inside the k -nearest neighbor ball, but it also has to be in alternating distances for the statistic to be minimal. From a risk management perspective a more relaxed measure is desirable because we do not want to generate datapoints that are too close to empirical ones but give the process some freedom to generate scenarios that have not happened in the past.

Additionally, in the “nearest neighbor coincidences” test, empirical data points surrounded by a lot of generated points can compensate for data points that are mostly surrounded by empirical points. This compensation can’t happen for the non covered ratio or the Wald-Wolfowitz test. As we want to have a fitting all over the distribution, this seems more desirable.

For the formal definition of the non-covered ratio, we first have to formally define the *nearest neighbor* and the *nearest neighbor distance*. For this, we recall definitions from Henze [1988], Zhou and Jammalamadaka [1993] and Ebner et al. [2018].

Remember that in Chapter 3.2, we defined the following sets of random variables $\mathbb{E}(\omega) = \{E_1(\omega), \dots, E_m(\omega)\}$ and $\mathbb{G}(\omega) = \{G_1(\omega), \dots, G_m(\omega)\}$ for each $\omega \in \Omega$ representing the empirical and generated data sets. Based on this, we define the following indices

$$\begin{aligned}\mathcal{E} &= \{1, \dots, m\} \\ \mathcal{G} &= \{m + 1, \dots, 2m\} \\ \mathcal{H} &= \{1, \dots, 2m\}\end{aligned}$$

and the random variable

$$H_i = \begin{cases} E_i & , 1 \leq i \leq m \\ G_{i-m} & , m + 1 \leq i \leq 2m \end{cases}$$

Let $|\cdot|$ be some norm on \mathbb{R}^d . We take the following definition of a *nearest neighbor* of a random variable from Henze [1988]:

Definition 1. Let $i \in \{1, \dots, 2m\}$. Let $r \in \mathbb{N}$. The k^{th} -nearest neighbor of a random variable H_i in the set $J \subset \{1, \dots, 2m\}$ is the random variable $N_k^J(H_i)$ defined by

$$N_k^J(H_i)(\omega) := H_j(\omega),$$

such that $j \in J \setminus i$ (j depends on ω) and

$$\forall l \in J \setminus i : |H_j(\omega) - H_i(\omega)| \leq |H_l(\omega) - H_i(\omega)|,$$

if $k = 1$ and

$$|H_l(\omega) - H_i(\omega)| < |H_j(\omega) - H_i(\omega)|$$

for exactly $k - 1$ values of $l, l \in J \setminus i$ if $k > 1$.

If $J = \{1, \dots, 2m\}$ we write N_k instead of N_k^J . If ties occur where two points have the same distance to another point, this occurs with probability zero and can be neglected. For further discussion on this issue of ties, we refer to Schilling [1986, p. 799] who uses a ranking in this case.

Based on this definition, we can now define the *nearest neighbor distance* as in Bickel and Breiman [1983]:

Definition 2. Let $i \in \{1, \dots, 2m\}$. Let $r \in \mathbb{N}$. The k^{th} -nearest neighbor distance of H_i in the set $J \subset \{1, \dots, 2m\}$ is defined by the random variable

$$R_k^J(H_i)(\omega) = |H_i(\omega) - N_k^J(H_i)(\omega)|$$

In particular, $R_1^J(H_i)(\omega) = \min_{j \in J \setminus i} |H_i - H_j|$.

With this definition, we can check for each random variable E_j if there is a random variable out of the generated set “quite close” to it which means nearer than the k -th nearest neighbour distance for some fixed $k \in \mathbb{N}$. Formally, we can define this as the non-covered ratio:

Definition 3. Let $\mathbb{E}(\omega) = \{E_1(\omega), \dots, E_m(\omega)\}$ and $\mathbb{G}(\omega) = \{G_1(\omega), \dots, G_m(\omega)\}$ for $\omega \in \Omega$ be sets of i.i.d. random variables as above with $m \in \mathbb{N}$. The *non-covered ratio* $NCR_{k,m}$ of \mathbb{G} with respect to \mathbb{E} for the k -nearest neighbors is then defined as

$$NCR_{k,m}(\mathbb{G}(\omega), \mathbb{E}(\omega)) = \frac{1}{m} \sum_{i=1}^m 1_{[R_k^{\mathbb{E}}(E_i)(\omega), \infty)} \left(\min_{j=1, \dots, m} |G_j(\omega) - E_i(\omega)| \right)$$

for some $k \in \mathbb{N}$ and $R_k^{\mathbb{E}}(E_i)(\omega)$ being the k -nearest neighbor distance of a random variable E_i in \mathbb{E} .

So this ratio is high if a lot of empirical data points do not have an generated datapoint in their nearest neighbourhood. The lower the ratio, the better the empirical data points are covered.

Analogously, one can define the measure

$$NCR_{k,m}(\mathbb{E}(\omega), \mathbb{G}(\omega)) = \frac{1}{m} \sum_{i=1}^m 1_{[R_k^{\mathbb{G}}(G_i)(\omega), \infty)} \left(\min_{j=1, \dots, m} |E_j(\omega) - G_i(\omega)| \right)$$

For the ease of reading, we will from now on skip the ω in the formulas. One could think of constructing a symmetric measure taking the average of $NCR_{k,m}(\mathbb{G}, \mathbb{E})$ and $NCR_{k,m}(\mathbb{E}, \mathbb{G})$. We don't do that for the following reason: The measure $NCR_{k,m}(\mathbb{G}, \mathbb{E})$ exactly detects “mode collapse”, the case where the generator only produces one single value or covers only parts of the distribution instead of generating a whole distribution. As this is an issue often occurring in

GAN training and has to be detected and avoided, see Motwani and Parmar [2020, Chapter 3.1] and Goodfellow [2016, Chapter 5.1.1], it is useful to have a specialized indicator for this case. The measure $NCR_{k,m}(\mathbb{E}, \mathbb{G})$, in contrast, detects if there are a lot of outliers being generated that are far away from the empirical data. If “mode collapse” occurs than the GAN architecture has to be restructured to get better results whereas in the latter case more training iterations can form a solution. Therefore, it’s useful to have a look at both measures separately.

If the distributions of E and G are the same, the non-covered ratio converges with the number of data points m increasing, as the following theorem shows. To derive this result, we first have to discuss the convergence of the expected value and the variance. For the sake of readability, we moved all proofs in the appendix.

Lemma 4. *Under the null hypothesis $H_0 : F_G = F_E$, the expected value of the non-covered ratio $E_{H_0}[NCR_{k,m}(\mathbb{G}, \mathbb{E})]$ converges and it holds*

$$\lim_{m \rightarrow \infty} E_{H_0}[NCR_{k,m}(\mathbb{G}, \mathbb{E})] = \frac{1}{2^k} \quad (4.1)$$

Lemma 5. *Under the null hypothesis $H_0 : F_G = F_E$, the sequence*

$$m \cdot \text{VAR}_{H_0}[NCR_{k,m}(\mathbb{G}, \mathbb{E})]$$

converges and it holds

$$\lim_{m \rightarrow \infty} m \cdot \text{VAR}_{H_0}[NCR_{k,m}(\mathbb{G}, \mathbb{E})] = \frac{1}{2^k} - \frac{1}{4^k}$$

This implies the convergence of the variance of the non-covered ratio

$$\lim_{m \rightarrow \infty} \text{VAR}_{H_0}[NCR_{k,m}(\mathbb{G}, \mathbb{E})] = 0 \quad (4.2)$$

With this preparatory work, we can proof the stochastic convergence of $NCR_{k,m}(\mathbb{G}, \mathbb{E})$ using Chebyshev’s inequality.

Theorem 6. *Let $NCR_{k,m}(\mathbb{G}, \mathbb{E})$ be the non-covered ratio as defined above and null hypothesis $H_0 : F_E = F_G$ holds. Then $NCR_{k,m}(\mathbb{G}, \mathbb{E})$ converges stochastically to $\frac{1}{2^k}$ for $m \rightarrow \infty$.*

4.3 Measure for the detection of the memorizing effect: memorizing ratio

All measures above will lead to optimal scores if the generated data points exactly match the empirical ones, so $\mathbb{E} = \mathbb{G}$ or show only tiny differences. This is not the optimal result because we want to create new scenarios which could have happened instead of memorizing scenarios that have actually taken place,

see Chen et al. [2018, p. 2]. Therefore, we need a measure to detect whether the generated data points really differ from the empirical ones and the GAN is not simply memorizing the data points (“overfitting”).

As in a multi-dimensional space it is highly unlikely for generated and empirical data points to match exactly, we extend the definition and classify a generated datapoint $G_j \in \mathbb{G}$ as being memorized if it lays in “an unusual small neighbourhood” around an empirical data point. We here define an “unusual small neighbourhood” as a fraction $0 < \rho \leq 1$ of the nearest neighbour distance of an empirical datapoint $E_i \in \mathbb{E}$ to the next empirical data point. If this is the case for a lot of $E_i \in \mathbb{E}$, than the generated dataset is not significantly differing from the empirical one. The memorizing ratio then describes the proportion of $E_i \in \mathbb{E}$ where the unwanted memorizing effect occurs.

This definition is also new to literature. The only existing test detecting memorizing in GANs which we found in literature is the birthday paradox test, see Borji [2019]. But this test is based on the visual identification of duplicates for pictures and therefore cannot be utilized in our context.

Definition 7. Let $\rho \in (0, 1]$. The *memorizing ratio* $MR_\rho(\mathbb{E}, \mathbb{G})$ is defined as:

$$MR_\rho(\mathbb{E}, \mathbb{G}) = \frac{1}{m} \sum_{i=1}^m \mathbf{1}_{[0, \rho \cdot R_{E_i}^1)} \left(\min_{j=1, \dots, m} |G_j - E_i| \right)$$

A graphical interpretation of the memorizing ratio can be found in Figure 4.3. In this example, E_n is the 1-nearest neighbor of E_i from the empirical set \mathbb{E} . The nearest neighbor distance between E_i and E_n is $R = |E_n - E_i|$. K_R then is the ball around E_i with radius R , whereas $K_{\rho R}$ forms the inner ball around E_i with radius ρR with $\rho \leq 1$. In the figure, the datapoint G_{j_3} counts as a memorized data point whereas G_{j_1} and G_{j_2} are not categorized as being memorized.

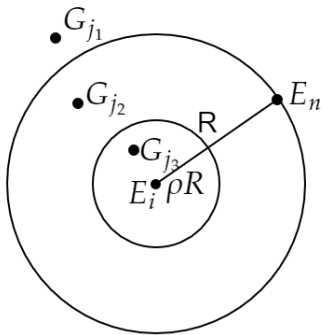


Figure 4.3: Visualization of the objects in the memorizing ratio context

For $\rho = 1$, there is a simple relationship between the non-covered ratio and the memorizing ratio and it holds:

$$MR_1(\mathbb{E}, \mathbb{G}) = 1 - NCR_{1,m}(\mathbb{G}, \mathbb{E})$$

It is clear that if $\lambda\%$ of the generated data points of \mathbb{G} are simply memorized data points from \mathbb{E} (meaning that $\lambda\%$ of the realisations from \mathbb{G} and \mathbb{E} are identical), then the expected value of the memorizing ratio $E[MR_\rho(\mathbb{E}, \mathbb{G})] > \lambda$. So, we can use this measure to test on the memorizing effect.

Under the null hypothesis of both distributions being the same, this measure also converges as the following theorem shows:

Theorem 8. *Under the null hypothesis $H_0 : F_G = F_E$, the expected value of the memorizing ratio $\mathbf{E}_{H_0}[MR_\rho(\mathbb{E}, \mathbb{G})]$ converges and it holds*

$$\lim_{m \rightarrow \infty} \mathbf{E}_{H_0}[MR_\rho(\mathbb{E}, \mathbb{G})] = \frac{\rho^d}{\rho^d + 1}$$

where $d \in \mathbb{N}$ is the dimension of the random vectors E and G .

This can be seen as the lower boundary of the memorizing ratio if the distributions are the same. Therefore, we use the difference of $MR_\rho(\mathbb{E}, \mathbb{G}) - \frac{\rho^d}{\rho^d + 1}$ for evaluation.

To check for the convergence empirically, we conducted a two-sample test for different values of ρ in various dimensions and with the same distribution for both samples. We conducted this test with different distributions (e.g. normal, exponential, student-t). We calculated the value of the memorizing ratio then for an increasing number of data points in each sample. Figure 4.4 presents the test for 2 dimensions, normal distributions and three different values for ρ .



Figure 4.4: Convergence test for the memorizing ratio

As expected, the memorizing ratio always converges to $\frac{\rho^d}{\rho^d+1}$. To derive the convergence speed, we can use the following definition from Leisen and Reimer [1996] :

Definition 9. A sequence of errors ϵ_N converges with order $\alpha > 0$, if there is a constant $\kappa > 0$ such that

$$\forall N \in \mathbb{N} : \epsilon_N \leq \frac{\kappa}{N^\alpha}$$

The order of convergence can be determined by simulation if we use, as in Leisen and Reimer [1996] or Junike [2019, Chapter 18.6], the transformation

$$\log\left(\frac{\kappa}{N^\alpha}\right) = \log(\kappa) - \alpha \log(N)$$

and perform a linear regression on the log-log-scale based on the data from the convergence test above. In our tests, we found the order of convergence to be between 0.02 and 0.6, strongly depending on ρ . The order of convergence is very low if ρ is small. Therefore, we suggest to use a value of at least 0.5 for ρ .

4.4 Hyperparameter optimization using these evaluation measures

In the preceding sections, we determined a combination of Wasserstein distance for each risk factor $w_i, i = 1, \dots, d$, both variants of the non-covered ratio $NCR_{k,m}(\mathbb{E}, \mathbb{G})$ (abbr. *ncr_b*) and $NCR_{k,m}(\mathbb{G}, \mathbb{E})$ (abbr. *ncr_o*) and the memorizing ratio $MR_\rho(\mathbb{E}, \mathbb{G})$ (abbr. *mr*) being useful to determine the quality of the GAN results.

We now want to use these evaluation measures to optimize the hyperparameters of the two neural networks and the GAN infrastructure itself. In a GAN, there is a lot of different variants to be tested. A full optimization is not possible as, see Motwani and Parmar [2020, Chapter 2], the “selection of the GAN model for a particular application is a combinatorial exploding problem with a number of possible choices and their orderings. It is computationally impossible for researchers to explore the entire space.” So, in our work, we check on the following:

- Number of layers for generator and discriminator: Not only the number itself, but also the relation between the number of layers in each neural network can make a big difference.
- Number of neurons per layer: This, too, can be different between the two neural networks and can also vary from layer to layer inside a network.
- Number of training iterations of the generator versus discriminator: The discriminator is usually trained k times in each iteration where the generator is trained once. We will check for an optimal parameter k .
- Dimension of the latent space: The latent space where the input for the generator is sampled usually has a higher dimensionality than the dimension of the generators’ output.
- Functions used in the GAN: The activation functions in the layers of the two networks, the optimisation algorithm and the usage of batch normalisation can be varied.

We performed our tests for $d=46$ dimensions and with the parameters $k = 3$ and $\rho = 0.7$. The data used was derived from the MCRCS study conducted by EIOPA (see EIOPA MCRCS Project Group [2020b]) and will be further discussed in Chapter 5.

Figure 4.5 shows the development of the Wasserstein distances for all 46 risk factors and the development of the other three measures with both neural networks having 4 layers over the 2500 training iterations:

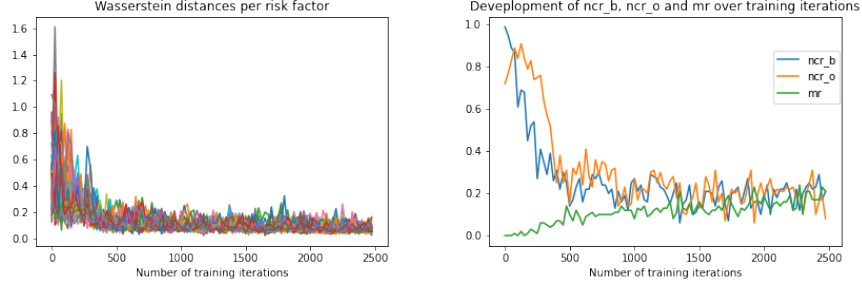


Figure 4.5: Development of the chosen GAN evaluation measures for the GAN with (4,4)-layer configuration

In the right figure, one can clearly see the behaviour of the memorizing ratio serving as an opponent to the non-covered ratio: Over the training iterations, the data distributions get closer and closer, and therefore the non-covered ratio decreases near to its expected value of $\frac{1}{2^3}$. The memorizing ratio, however, increases with more training iterations. The expected value of the memorizing ratio in this case is close to zero ($\frac{0.7^{46}}{0.7^{46}+1} \approx 10^{-8}$). In this configuration, about a fifth of the data points at the end of the training is classified as being memorized. However, a large number of memorized points is undesirable. Therefore, the omittance of this ratio would lead to the selection of a non-optimal GAN architecture.

To derive at one value for the total performance of the GAN architecture in question, we have to aggregate the values from the four measures in each evaluation run. Our experience shows that simply taking the average of the four measures as the target function tf works well. In other contexts, it can make sense to introduce some kind of weighting in this formula.

$$tf = \frac{1}{4} \left(\max_{i=1, \dots, 46} (w_i) + |ncr_o - \frac{1}{2^k}| + |ncr_b - \frac{1}{2^k}| + \max(mr - \frac{\rho^d}{\rho^d + 1}, 0) \right)$$

The measures for the differences between joint distributions (ncr_b and ncr_o) and mr can be evaluated in a space with the same dimension as the input parameters, so one figure per measure is obtained. For ncr_o and ncr_b, we subtract the expected value under the null hypothesis of equal distributions and take the absolute value. For mr, we take the maximum of the absolute value of the difference between mr and their expected value under the null hypothesis and 0 because lower values for mr mean a lower amount of memorized data points which is not only accepted but appreciated. The Wasserstein distance, however, is determined for each risk factor, in our case leading to 46 figures. To aggregate, we will use the maximum over this 46 risk factors, leading to one figure for Wasserstein, too.

Figure 4.6 demonstrates the development of the tf -value over the training iterations for a configuration with both neural networks having 4 layers. As it is computationally expensive to calculate this tf -value in every iteration of the GAN training, we decide to determine the tf -value every 25 training iterations where 25 is a compromise between accuracy and computational feasibility.

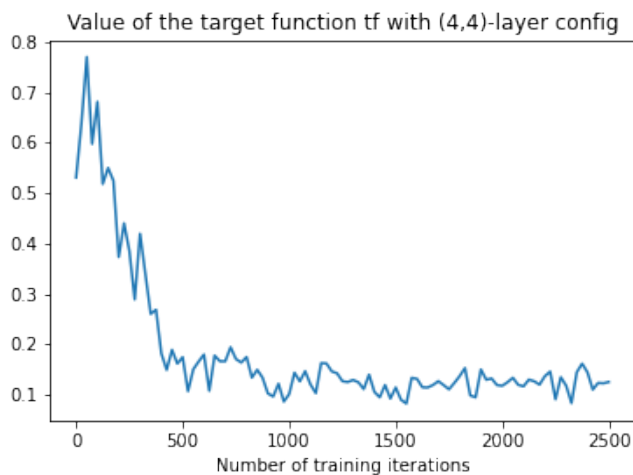


Figure 4.6: Development of the tf -value for a GAN with a (4,4)-layer configuration

Based on the tf -value, one can then select not only the best architecture, but also the optimal number of training iterations.

In the experiments, one can clearly see that the GAN is not converging but there is a minimum of the target function during training and afterwards the tf -value starts increasing again. This is the behaviour typically seen in GAN training, see e.g. Goodfellow [2016, p. 34]. Figure 4.7 displays the Wasserstein (left) and $ncr_o/ncr_b/mr$ -measures (right) for a run with 5000 iterations:

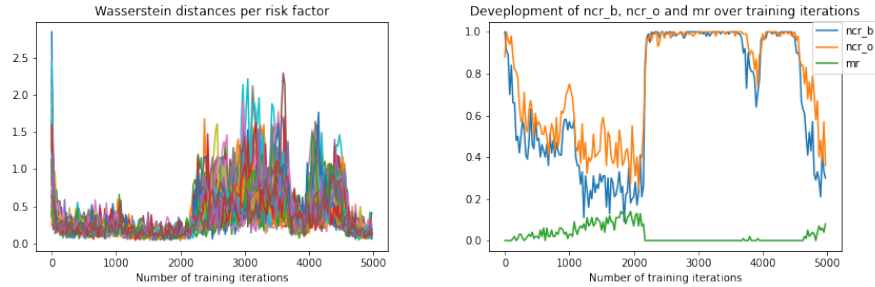


Figure 4.7: Development of the chosen GAN evaluation measures over 5000 training iterations

Based on our analysis of 50 different settings, we use the following configuration for our GAN-based ESG:

- 4 layers for discriminator and generator
- 400 neurons per layer in the discriminator and 200 in the generator
- 10 training iterations for the generator in each discriminator training
- Dimension of the latent space is 200
- We use LeakyReLU as activation functions, except for the output layers which use sigmoid (for discriminator) and linear (for generator) activation functions. We use the Adam optimizer and batch normalisation after each of the layers in the network.

For this GAN, we check at which iteration the tf -value is minimized. In our case, this is iteration 2425. Then we use the trained generator at this iteration to generate the scenarios for our comparison with the results of classical ESGs in the next chapter.

5 Comparison of GAN results with the results of the MCRCS study

5.1 Introduction to the MCRCS study

Since 2017, the “European Insurance and Occupational Pensions Authority” EIOPA performs an annual study, called the *market and credit risk comparison study*, abbr. "MCRCS". According to the instructions from EIOPA MCRCS Project Group [2020b], the "primary objective of the MCRCS is to compare market and credit risk model outputs for a set of realistic asset portfolios". In the study, all insurance undertakings with significant exposure in EUR and with an approved internal model are asked to participate, see EIOPA MCRCS

Project Group [2021]. In the study as of year-end 2019, 21 insurance companies from 8 different countries of the European Union participated.

All participants are asked by their local regulators to model the risk of 104 different synthetic instruments. Those comprise all relevant asset classes, i.e. risk-free interest rates, sovereign bonds, corporate bonds, foreign exchange rates, equity indices, property, foreign exchange and some derivatives. A detailed overview of the synthetic instruments that are used in this study can be found in EIOPA MCRCS Project Group [2020a].

Additionally, those instruments are grouped into 10 different asset-only benchmark portfolios, 2 liability-only benchmark portfolios and 10 combined portfolios. These portfolios "should reflect typical asset risk profiles of European insurance undertakings", see EIOPA MCRCS Project Group [2020b, Section 2]. This analysis sheds light into the interaction and dependencies between the risk factors. Figure 5.1 presents the asset-type composition of the asset-only benchmark portfolios.

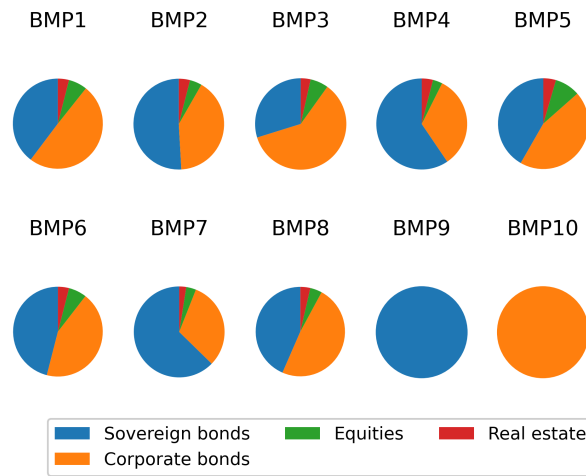


Figure 5.1: Composition of the MCRCS benchmark portfolios BMP1 - BMP10

All asset portfolios mainly consist of fixed income securities (86% to 94%) as this forms the main investment focus of insurance companies. However, there are significant differences both in ratings, durations and also in the weighting between sovereign and corporate exposures. The two liability profiles are assumed to be zero-bond based, so they represent a non-life insurance companies' liabilities and differ in their durations (13.1 years vs. 4.6 years).

5.2 Methodology and data

For the purpose of this article, we will only compare the risk charges for instruments that are also included in the benchmark portfolios. An aggregated view of these instruments together with the used Bloomberg sources can be found in Appendix D. As the study used here is at year-end 2019, we take the datapool from end of March 2002 until Dec. 2019 as the basis of our GAN training. We therefore have 4587 daily observations in this dataset which comprises almost 18 years.

In Solvency 2, we have to model the market risk for a one year horizon. There are two approaches to derive the risk based on higher frequent data (here daily returns) for a longer horizon (here annually). One solution is to use the daily data to train the GAN model and then use some autocorrelation function to generate an annual time series based on daily returns. The other solution is to use overlapping rolling windows of annual returns on a daily basis for the training of the model. The first method is covered in Fu et al. [2019]. We will in this work use overlapping rolling windows as explained in Wiese et al. [2020, p. 16] and EIOPA MCRCS Project Group [2021, p. 17].

Annually, EIOPA provides a detailed study with a comparison of the results by BMP, instruments and some additional analysis, e.g. for the analysis of dependencies for the risk factors. The study for year-end 2019 can be found on the EIOPA homepage, see EIOPA MCRCS Project Group [2021]. There, the risk charges are compared between the participating insurance companies in an anonymized way.

5.3 Comparison on risk-factor level

The results on risk factor basis are analyzed based on the shocks generated or implied by the ESGs. A shock hereby is defined in EIOPA MCRCS Project Group [2021, p. 11] as

Definition 10. A shock is the absolute change of a risk factor over a one-year time horizon. Depending on the type of risk factor, the shocks can either be two-sided (e.g. interest rates ‘up/down’) or one-sided (e.g. credit spreads ‘up’). This metric takes into account the undertakings’ individual risk measure definitions (in particular whether the mean of the distribution is taken into account or not) and is based on the 0.5% and 99.5% quantiles for two-sided risk factors and the 99.5% quantile for one-sided risk factors, respectively.

The results are presented in one diagram, showing boxes with whiskers for each maturity / sub-type of this risk factor. The boxes contain the shocks of the participating insurance companies between the 25%- and 75%-percentile of all participants. The whiskers extend this to the 10%- and 90%-percentile. The sample consists of 21 participants at maximum; results are only provided if an

insurance company states at least some exposure to this risk-factor.

We enrich those results with a blue dot representing the shock for that risk factor generated by our GAN-based model. In this work, we will show the comparison of the four most important risk factor shocks (interest rate up and down, credit spread and equity).

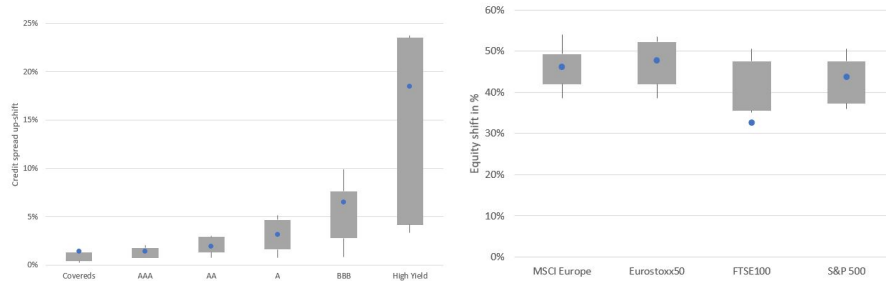


Figure 5.2: Comparison of the simulated shifts for the credit spread and equity risk factors, representation based on own results and EIOPA MCRCS Project Group [2021, p. 25 and 27]

For credit spreads and equity, Figure 5.2, we see a good alignment between the GAN-based model and the approved internal models. On the equity side, the alignment is also good for most of the risk factors. For the FTSE100, the GAN produces less severe shocks than the other models. This behaviour, however, can actually be found in the training data as the FTSE100 is less volatile than the other indices for the time frame used in GAN training. So, the GAN here produces plausible results.

For interest rates, however, the picture is more complex as Figure 5.3 illustrates:

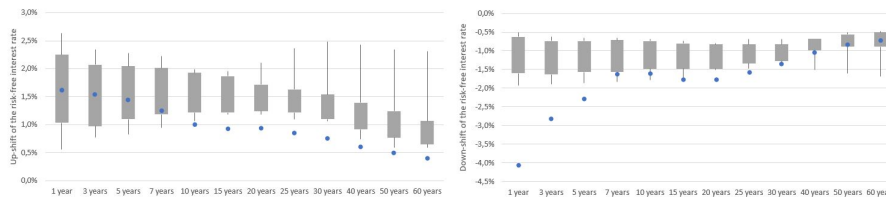


Figure 5.3: Comparison of the simulated shifts for the most important risk factors, representation based on own results and EIOPA MCRCS Project Group [2021, p. 22]

The up-shifts generated by the GAN-based model are within the boxes (25%-percentile to 75%-percentile of the participating internal models) for 1 to 7 year

buckets. Afterwards, the shifts are below the whiskers. This effect is probably due to the time span of the data used for the training of the GAN. The interest rates in this time period (Mar. 2002 - Dec. 2019) are mostly decreasing. In the traditional ESGs, the interest rates are probably calibrated on a longer horizon so they include upward trends in long term interest rates from a longer history. We use this time horizon in our GAN training since the availability of consistent market data gets more difficult if one goes further back in history.

For the down-shifts, the graph shows a contrary behaviour: The short- and medium term interest rates are far below the whiskers, whereas the longer term interest rates mostly are inside the whiskers or boxes. This also can be explained by the interest rate development: The time span used for training of the GAN shows a sharp decrease of interest rates especially in the short term whereas longer term interest rates behaved more stable. This behaviour is mimicked by the GAN. In traditional ESGs, additionally to the longer time span used for calibration, often expert judgement by the insurers leads to a lower bound on how negative interest rates can become.

If an insurance company wants to include more up-shifts in the training, the training data has to be transformed accordingly. This, however, would deviate from the idea of the GAN-based ESG as a full data-driven model. Additionally, it is a valid point to discuss whether the interest rate movements having occurred in a different regime with much higher interest rates are meaningful for the fluctuations in a current low interest rate environment.

5.4 Comparison on portfolio level

The main comparison between the results for the the benchmark portfolios is based on the "risk charge" which is defined in EIOPA MCRCS Project Group [2020b, Section 2].

Definition 11. The *risk charge* is the ratio of the modelled Value at Risk (99.5%, one year horizon) and the provided market value of the portfolio.

In this work, we only show the comparison of the risk charges for the combined asset-and-liabilities portfolios. The comparisons for asset-only and liability-only benchmark portfolios follow a similiar pattern.

Figure 5.4 displays for each of the benchmark portfolios which comprises the longer liability structure (left) or the shorter liabilities (right) the risk charge of this portfolio. As in the comparison for the risk factors, the grey boxes contain the risk charges of the participating insurance companies between the 25%- and 75%-percentile. The whiskers extend this to the 10%- and 90%-percentile. The sample consists of 21 participants, so 4 results (2 above, 2 below the whiskers) are not shown. The risk charge according to our GAN-based model is repre-

sented by a blue dot.

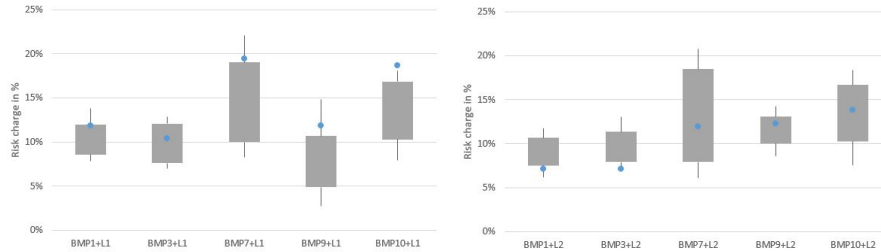


Figure 5.4: Comparison of the combined asset-liability benchmark portfolios, representation based on own results and EIOPA MCRCs Project Group [2021, p. 14]

The risk charge of the GAN-based model fits well to the risk charges of the established models. On the left side (longer liability structure), the blue dot always is in the upper percentile of the risk charges or slightly above the 90%-percentile. Due to the asset-liability duration profile in this portfolio, the risk charge is generated by scenarios with decreasing interest rates. In the risk factor comparison of the interest rate down shock, the interest rate down shifts are more severe in most maturities for the GAN-based model than for the classical models. Therefore, it seems plausible for the resulting portfolio risk to be at the upper percentiles, too.

The right graph (shorter liability structure) shows a bit a different picture: The risk charge of the GAN-based model mostly lies within the boxes or within the lower whiskers. This is due to the fact that for this portfolio structure, increasing interest rates form a main risk. As the shocks for the GAN-based model for increasing interest rates are within the boxes or even below the boxes, this behaviour can be explained, too.

Overall, the resulting risk charges for the GAN-based model are comparable to the results of the approved internal models in Europe. Therefore, GAN-based models can be seen as an appropriate alternative way of market risk modelling.

6 Summary and Conclusion

In this research, we have shown how a generative adversarial network (GAN) can serve as an economic scenario generator (ESG). Compared to the current approaches, a GAN-based ESG is an assumption-free approach that can model complex dependencies between risk factors.

For validation purposes as well as for the optimization of the GAN itself, we provided three measures that can evaluate the performance of the scenario generation of the GAN: Wasserstein distance (measuring the alignment of the distributions of the risk factors), non-covered ratio (measuring the alignment of the dependencies between the risk factors and controlling mode-collapse) and the memorizing ratio (measuring overfitting). We provided a framework how these measures can be used in the hyperparameter and GAN architecture optimization process.

Finally, we showed that the results of a GAN-based ESG are comparable to the currently used ESGs when using the EIOPA MCRCs study as a benchmark.

Acknowledgement 12. S. Flaig would like to thank Deutsche Rückversicherung AG for the funding of this research. Opinions, errors and omissions are solely those of the authors and do not represent those of Deutsche Rückversicherung AG or its affiliates.

References

- Alankrita Aggarwal, Mamta Mittal, and Gopi Battineni. Generative adversarial network: An overview of theory and applications. *International Journal of Information Management Data Insights*, page 100004, 2021.
- Christoph Bennemann. *Handbuch Solvency II: von der Standardformel zum internen Modell, vom Governance-System zu den MaRisk VA*. Schäffer-Poeschel, 2011.
- Peter J Bickel and Leo Breiman. Sums of functions of nearest neighbor distances, moment bounds, limit theorems and a goodness of fit test. *The Annals of Probability*, pages 185–214, 1983.
- Ali Borji. Pros and cons of gan evaluation measures. *Computer Vision and Image Understanding*, 179:41–65, 2019.
- Yize Chen, Pan Li, and Baosen Zhang. Bayesian renewables scenario generation via deep generative networks. In *2018 52nd Annual Conference on Information Sciences and Systems (CISS)*, pages 1–6. IEEE, 2018.
- Francois Chollet et al. *Deep learning with Python*, volume 361. Manning New York, 2018.
- Thomas Cover and Peter Hart. Nearest neighbor pattern classification. *IEEE transactions on information theory*, 13(1):21–27, 1967.
- DAV. Zwischenbericht zur Kalibrierung und Validierung spezieller ESG unter Solvency II. Ergebnisbericht des Ausschusses Investment der Deutschen Aktuarvereinigung e.V., 2015. URL <https://aktuar.de/unsere-themen/>

- fachgrundsätze-oeffentlich/2015-11-09_DAV-Ergebnisbericht_Kalibrierung_und_Validierung_spezieller_ESG_Update.pdf.
- Michel Denuit, Jan Dhaene, Marc Goovaerts, and Rob Kaas. *Actuarial theory for dependent risks: measures, orders and models*. John Wiley & Sons, 2006.
- Bruno Ebner, Norbert Henze, and Joseph E Yukich. Multivariate goodness-of-fit on flat and curved spaces via nearest neighbor distances. *Journal of Multivariate Analysis*, 165:231–242, 2018.
- Florian Eckerli. Generative adversarial networks in finance: an overview. *Available at SSRN 3864965*, 2021.
- EIOPA. The underlying assumptions in the standard formula for the solvency capital requirement calculation. *the European Insurance and Occupational Pensions Authority*, 2014.
- EIOPA MCRCS Project Group. 13.01.2020_MCRCS 2019 instruments and BMP.xlsx, 2020a. URL https://www.eiopa.europa.eu/sites/default/files/toolsanddata/mcrs_2019_instruments_and_bmp.xlsx.
- EIOPA MCRCS Project Group. YE2019 Comparative Study on Market and Credit Risk Modelling, 2020b. URL https://www.eiopa.europa.eu/sites/default/files/toolsanddata/mcrs_year-end_2019_instructions_covidpostponed.pdf.
- EIOPA MCRCS Project Group. YE2019 Comparative Study on Market and Credit Risk Modelling, 2021. URL https://www.eiopa.europa.eu/sites/default/files/publications/reports/2021-study-on-modelling-of-market-and-credit-risk_mcrs.pdf.
- European Union. Commission delegated regulation (EU) 2015/35 of 10 October 2014 supplementing directive 2009/138/EC of the European parliament and of the council on the taking-up and pursuit of the business of insurance and reinsurance (Solvency II). *Official Journal of European Union*, 2015.
- Jerome H Friedman and Lawrence C Rafsky. Multivariate generalizations of the wald-wolfowitz and smirnov two-sample tests. *The Annals of Statistics*, pages 697–717, 1979.
- Rao Fu, Jie Chen, Shutian Zeng, Yiping Zhuang, and Agus Sudjianto. Time series simulation by conditional generative adversarial net. *arXiv preprint arXiv:1904.11419*, 2019.
- Ian Goodfellow. Nips 2016 tutorial: Generative adversarial networks. *arXiv preprint arXiv:1701.00160*, 2016.
- Ian Goodfellow, J. Pouget-Abadie, and M. et al Mirza. Generative adversarial nets. *Advances in neural information processing systems*, pages 2672–2680, 2014.

- Marc Hallin, Gilles Mordant, and Johan Segers. Multivariate goodness-of-fit tests based on wasserstein distance. *Electronic Journal of Statistics*, 15(1): 1328–1371, 2021.
- Pierre Henry-Labordere. Generative models for financial data. *Available at SSRN 3408007*, 2019.
- Norbert Henze. A multivariate two-sample test based on the number of nearest neighbor type coincidences. *The Annals of Statistics*, 16(2):772–783, 1988.
- Gero Quintus Rudolf Junike. *Advanced stock price models, concave distortion functions and liquidity risk in finance*. 2019.
- Dietmar PJ Leisen and Matthias Reimer. Binomial models for option valuation—examining and improving convergence. *Applied Mathematical Finance*, 3(4): 319–346, 1996.
- Edmond Lezmi, Jules Roche, Thierry Roncalli, and Jiali Xu. Improving the robustness of trading strategy backtesting with boltzmann machines and generative adversarial networks. *Available at SSRN 3645473*, 2020.
- Ziqiang Li, Rentuo Tao, and Bin Li. Regularization and normalization for generative adversarial networks: A review. *arXiv preprint arXiv:2008.08930*, 2020.
- Pronoy K Mondal, Munmun Biswas, and Anil K Ghosh. On high dimensional two-sample tests based on nearest neighbors. *Journal of Multivariate Analysis*, 141:168–178, 2015.
- Tanya Motwani and Manojkumar Parmar. A novel framework for selection of gans for an application. *arXiv preprint arXiv:2002.08641*, 2020.
- Hao Ni, Lukasz Szpruch, Magnus Wiese, Shujian Liao, and Baoren Xiao. Conditional sig-wasserstein gans for time series generation. *arXiv preprint arXiv:2006.05421*, 2020.
- Dietmar Pfeifer and Olena Ragulina. Generating VaR scenarios under Solvency II with product beta distributions. *Risks*, 6(4):122, 2018.
- Aaditya Ramdas, Nicolás García Trillos, and Marco Cuturi. On wasserstein two-sample testing and related families of nonparametric tests. *Entropy*, 19(2):47, 2017.
- Eitan Richardson and Yair Weiss. On gans and gmms. *arXiv preprint arXiv:1805.12462*, 2018.
- Mark F Schilling. Multivariate two-sample tests based on nearest neighbors. *Journal of the American Statistical Association*, 81(395):799–806, 1986.

Magnus Wiese, Lianjun Bai, Ben Wood, and Hans Buehler. Deep hedging: learning to simulate equity option markets. *arXiv preprint arXiv:1911.01700*, 2019.

Magnus Wiese, Robert Knobloch, Ralf Korn, and Peter Kretschmer. Quant gans: Deep generation of financial time series. *Quantitative Finance*, 20(9): 1419–1440, 2020.

Sean Zhou and S Rao Jammalamadaka. Goodness of fit in multidimensions based on nearest neighbour distances. *Journal of Nonparametric Statistics*, 2(3):271–284, 1993.

Appendix

A Proof of Lemma 4

Proof. If all of the k -nearest neighbours of a given E_i belong to the same sample as E_i , then via definition the distance of E_i to all G_j is greater than $R_{E_i}^k$. With the definition of the nearest neighbor NN_i^k and the indicator function $\mathbf{1}_{E_i}(r)$ above, we can do the following transformations for a given E_i and some $k \in \mathbb{N}$:

$$\begin{aligned} \mathbf{1}_{(R_{E_i}^k, \infty)}\left(\min_{j=1, \dots, m} \|G_j - E_i\|\right) &= 1 \\ \iff \forall j = 1, \dots, m : \|E_i - G_j\| &\geq R_{E_i}^k \\ \iff \forall r \leq k : NN_i^r \text{ belongs to the same sample as } E_i & \\ \iff \forall r \leq k : \mathbf{1}_{E_i}(r) = 1 & \end{aligned}$$

In the following, we use the notation P_{H_0} to indicate the probability under the null hypothesis H_0 . This means that $E_1, \dots, E_m, G_1, \dots, G_m$ are i.i.d. random variables. The number of realizations in $\mathcal{E} \cup \mathcal{G}$ is $2m$. So, for a given E_i , the k -nearest neighbor is one of the $2m - 1$ remaining sample random variables in $\mathcal{E} \cup \mathcal{G}$. So, the probability P_{H_0} that the random variable NN_i^r is from the same sample as E_i is $\frac{m-1}{2m-1}$ for a given r . Due to combinatorial considerations and with the fact that NN_i^r are independent random variables, the probability that all of the k -nearest neighbors of E_i belong to the same sample can be derived

iteratively, as in Schilling [1986, Proof of Theorem 3.1]:

$$\begin{aligned}
P_{H_0}[\mathbf{1}_{E_i}(1) = 1] &= \frac{m-1}{2m-1} \\
P_{H_0}[\mathbf{1}_{E_i}(1) = 1 \wedge \mathbf{1}_{E_i}(2) = 1] &= \frac{m-1}{2m-1} \cdot \frac{m-2}{2m-2} \\
&\vdots \\
P_{H_0}[\forall r \leq k : \mathbf{1}_{E_i}(r) = 1] &= \frac{(m-1) \cdots (m-k)}{(2m-1) \cdots (2m-k)} \\
&:= \alpha_{k,m}
\end{aligned}$$

With the transformation above, we can calculate the expected value under H_0 :

$$\begin{aligned}
\mathbf{E}_{H_0}[NCR_{k,m}(\mathcal{G}, \mathcal{E})] &= \frac{1}{m} \sum_{i=1}^m \mathbf{E}_{H_0} \left[\mathbf{1}_{[R_{E_i}^k, \infty)} \left(\min_{j=1, \dots, m} \|G_j - E_i\| \right) \right] \\
&= \frac{1}{m} \sum_{i=1}^m P_{H_0}[\forall r \leq k : \mathbf{1}_{E_i}(r) = 1] \\
&= \frac{1}{m} \sum_{i=1}^m \alpha_{k,m} \\
&= \alpha_{k,m}
\end{aligned}$$

For $m \rightarrow \infty$, every of the k factors of $\alpha_{k,m}$ converges to $\frac{1}{2}$:

$$\begin{aligned}
\lim_{m \rightarrow \infty} \mathbf{E}_{H_0}[NCR_{k,m}(\mathcal{G}, \mathcal{E})] &= \lim_{m \rightarrow \infty} \alpha_{k,m} \\
&= \frac{1}{2^k}
\end{aligned}$$

□

B Proof of Lemma 5

Proof. With the knowledge from the proof and the notations above, we can calculate:

$$\begin{aligned}
VAR_{H_0}[NCR_{k,m}(\mathcal{G}, \mathcal{E})] &= \mathbf{E}_{H_0}[NCR_{k,m}(\mathcal{G}, \mathcal{E})^2] - \mathbf{E}_{H_0}[NCR_{k,m}(\mathcal{G}, \mathcal{E})]^2 \\
&= \mathbf{E}_{H_0} \left[\frac{1}{m^2} \sum_{i=1}^m \sum_{l=1}^m \mathbf{1}_{[R_{E_i}^k, \infty)} \left(\min_{j=1, \dots, m} \|G_j - E_i\| \right) \right. \\
&\quad \left. \cdot \mathbf{1}_{[R_{E_l}^k, \infty)} \left(\min_{j=1, \dots, m} \|G_j - E_l\| \right) \right] \\
&\quad - \left(\alpha_{k,m} \right)^2
\end{aligned}$$

We can simplify the first term, if we differentiate between the summands where $i = l$ and where $i \neq l$. For $i = l$ the first term can be rewritten as:

$$\begin{aligned} & \sum_{i=1}^m \mathbf{1}_{[R_{E_i}^k, \infty)} \min_{j=1, \dots, m} \|G_j - E_i\| \cdot \mathbf{1}_{[R_{E_i}^k, \infty)} \left(\min_{j=1, \dots, m} \|G_j - E_i\| \right) \\ &= \sum_{i=1}^m \mathbf{1}_{[R_{E_i}^k, \infty)} \left(\min_{j=1, \dots, m} \|G_j - E_i\| \right) \end{aligned}$$

The $m(m-1)$ summands where $i \neq l$ can also be rewritten because E_i and E_l are independent

$$\begin{aligned} & \mathbf{1}_{[R_{E_i}^k, \infty)} \left(\min_{j=1, \dots, m} \|G_j - E_i\| \right) \cdot \mathbf{1}_{[R_{E_l}^k, \infty)} \left(\min_{j=1, \dots, m} \|G_j - E_l\| \right) \\ & \iff \forall r \leq k : \mathbf{1}_{E_i}(r) = 1 \text{ and } \mathbf{1}_{E_l}(r) = 1 \end{aligned}$$

With the same combinatorial arguments as above, one can calculate

$$\begin{aligned} & P_{H_0}[\mathbf{1}_{[R_{E_i}^k, \infty)} \left(\min_{j=1, \dots, m} \|G_j - E_i\| \right) \cdot \mathbf{1}_{[R_{E_l}^k, \infty)} \left(\min_{j=1, \dots, m} \|G_j - E_l\| \right)] \\ &= \left(\frac{(m-1) \cdots (m-k)}{(2m-1) \cdots (2m-k)} \right)^2 \\ &= \alpha_{k,m}^2 \end{aligned}$$

And this leads to

$$\begin{aligned} m \cdot \text{VAR}_{H_0}[NCR_{k,m}(\mathcal{G}, \mathcal{E})] &= \frac{m}{m^2} \left[\sum_{i=1}^m \mathbf{E}_{H_0}[\mathbf{1}_{[R_{E_i}^k, \infty)} \min_{j=1, \dots, m} \|G_j - E_i\| \right. \\ & \quad \left. + \mathbf{E}_{H_0} \left[\sum_{i=1}^m \sum_{l=1, \dots, m}^{l \neq i} \mathbf{1}_{[R_{E_i}^k, \infty)} \min_{j=1, \dots, m} \|G_j - E_i\| \right. \right. \\ & \quad \left. \left. \cdot \mathbf{1}_{[R_{E_l}^k, \infty)} \min_{j=1, \dots, m} \|G_j - E_l\| \right] \right] \\ & \quad - m \cdot (\alpha_{k,m})^2 \\ &= \frac{1}{m} \left[m \cdot \alpha_{k,m} + m(m-1) \cdot \alpha_{k,m}^2 \right] - m\alpha_{k,m}^2 \\ &= \alpha_{k,m} + m\alpha_{k,m}^2 - \alpha_{k,m}^2 - m\alpha_{k,m}^2 \\ &= \alpha_{k,m} - \alpha_{k,m}^2 \end{aligned}$$

We know that $\alpha_{k,m} \rightarrow \frac{1}{2^k}$ for $m \rightarrow \infty$ and therefore:

$$\lim_{m \rightarrow \infty} m \cdot \text{VAR}_{H_0}[NCR_{k,m}(\mathcal{G}, \mathcal{E})] = \frac{1}{2^k} - \frac{1}{4^k}$$

□

C Proof of Theorem 8

Proof. To be completed. □

D Table of instruments used for the MCRCS study

Here is the ticker list from Bloomberg for the data used for the market risk scenario generation:

Asset Class	Subtype	Maturity	Bloomberg ticker
Government Bond	Austria	5, 10 years	GTATS5Y/10Y Govt
	Belgium	5, 10 years	GTBEF5Y/10Y Govt
	Germany	5, 10 years	GTDEM5Y/10Y Govt
	Spain	5, 10 years	GTESP5Y/10Y Govt
	France	5, 10 years	GTFRF5Y/10Y Govt
	Ireland	5, 10 years	GIGB5Y/10Y Index
	Italy	5, 10 years	GTITL5Y/10Y Govt
	Netherlands	5, 10 years	GTNLG5Y/10Y Govt
	Portugal	5 years	GSPT5YR Index
	UK	5 years	C1105Y Index
US	5 years	H15T5Y Index	
Covered Bond	issued by AA-rated bank	5, 10 years	C9235Y/C92310Y Index
Corporate Bond	senior unsecured bond, rating AA	5, 10 years	C6675Y/C66710Y Index
Corporate Bond	senior unsecured bond, rating A	5, 10 years	C6705Y/C67010Y Index
Corporate Bond	senior unsecured bond, rating BBB	5, 10 years	C6735Y/C67310Y Index
Risk-free Interest Rates	EUR	1, 3, 5, 7, 10, 15, 20, 25, 30, 40, 50 years	S0045Z 1Y/.../50Y BLC2 Curncy
	USD	5 years	USSW5 Index
	GBP	5 years	BPSW5 Index
Equity Index	EuroStoxx50	-	SX5T Index
	MSCI Europe	-	MSDEE15N Index
	FTSE100	-	TUKXG Index
	S&P500	-	SPTR500N Index

Asset Class	Subtype	Maturity	Bloomberg ticker
Commercial real-estate	In Europe	-	EXUK Index